JACS
JOURNAL OF THE AMERICAN CHEMICAL SOCIETY
Article
pubs.acs.org/JACS

Supramolecular Self-Assembly Induced Adjustable Multiple Gating States of Nanofluidic Diodes

Ruochen Fang,[†,‡] Huacheng Zhang,[∥,‡] Liulin Yang,[†] Huanting Wang,[∥] Ye Tian,[*,§] Xi Zhang,[*,†] and Lei Jiang[*,∥,⊥]

[†]Key Lab of Organic Optoelectronics and Molecular Engineering, Department of Chemistry, Tsinghua University, Beijing 100084, People's Republic of China

[⊥]Key Laboratory of Bio-inspired Materials and Interfacial Science, Technical Institute of Physics and Chemistry, Chinese Academy of Sciences, Beijing 100190, People's Republic of China

[§]Beijing National Laboratory for Molecular Sciences, Key Laboratory of Green Printing, Institute of Chemistry, Chinese Academy of Sciences, Beijing 100190, People's Republic of China

[∥]Department of Chemical Engineering, Monash University, Clayton, Victoria 3800, Australia

Supporting Information

ABSTRACT: Artificial nanochannels, inheriting smart gating functions of biological ion channels, promote the development of artificial functional nanofluidic devices for high-performance biosensing and electricity generation. However, gating states of the artificial nanochannels have been mainly realized through chemical modification of the channels with responsive molecules, and their gating states cannot be further regulated once the nanochannel is modified. In this work, we employed a new supramolecular layer-by-layer (LbL) self-assembly method to achieve reversible and adjustable multiple gating features in nanofluidic diodes. Initially, a self-assembly precursor was modified into a single conical nanochannel, then host molecule-cucurbit[8]uril (CB[8]) and guest molecule, a naphthalene derivative, were self-assembled onto the precursor through an LbL method driven by host-enhanced $\pi-\pi$ interaction, forming supramolecular monolayer or multilayers on the inner surface of the channel. These self-assemblies with different layer numbers possessed remarkable charge effects and steric effects, exhibiting a capability to regulate the surface charge density and polarity, the effective diameter, and the geometric asymmetry of the single nanochannel, realizing reversible gating of the single nanochannel among multiple rectification and ion-conduction states. As an example of self-assembly of supramolecular networks in nanoconfinements, this work provides a new approach for enhancing functionalities of artificial nanochannels by LbL supramolecular self-assemblies. Meanwhile, since the host molecule, CB[8], used in this work can interact with different kinds of biomolecules and stimuli-responsive chemical species, this work can be further extended to build a novel stable multiple-state research platform for a variety of uses such as sensing and controllable release.

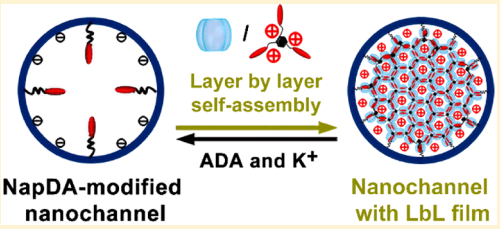

INTRODUCTION

Abiotic inorganic and polymeric nanochannels have attracted increasing research attention owing to their outstanding ability to control and manipulate the transport of ions and molecules flowing through them, thus enabling the construction of nanofluidic devices capable of sensing or separating diverse chemical species in aqueous solutions.[1−6] In the past decade, through covalently grafting a monolayer of stimuli-responsive molecules on the channel walls via various chemical modification methods, artificial nanochannels have been shown to display a series of smart gating functions that resemble biological protein channels, such as pH,[7−10] ion,[11−13] voltage,[14−18] temperature[19,20] and light responsiveness,[21,22] molecular sensing,[23−28] and so on.[29−33] However, because the gating processes of these covalently modified nanochannels are strictly dependent on the monolayer of responsive molecules, their application ranges of gating states cannot be further regulated once the nanochannels are modified. To adapt to various application conditions, it is important to realize reversible and adjustable multiple gating states of nanochannels; different gating states can correspond to different uses, such as sensing of proteins with different sizes, which can realize multifunctions in one nanochannel and promote the application of artificial nanofluidic devices.

Supramolecular self-assembly on surface has promoted the application of supramolecular architectures from solution to solid phases.[34−41] In a process of supramolecular self-assembly on surfaces, driving force and self-assembly method determine the properties and functions of the supramolecular architectures. Host-enhanced $\pi-\pi$ interaction combines host−guest interaction and $\pi-\pi$ interaction; a cucurbit[8]uril (CB[8])-based host-enhanced $\pi-\pi$ interaction can work in an aqueous environment with a two-step binding constant as high as 10^{12}

Received: September 13, 2016
Published: November 23, 2016

DOI: 10.1021/jacs.6b09601
J. Am. Chem. Soc. 2016, 138, 16372−16379

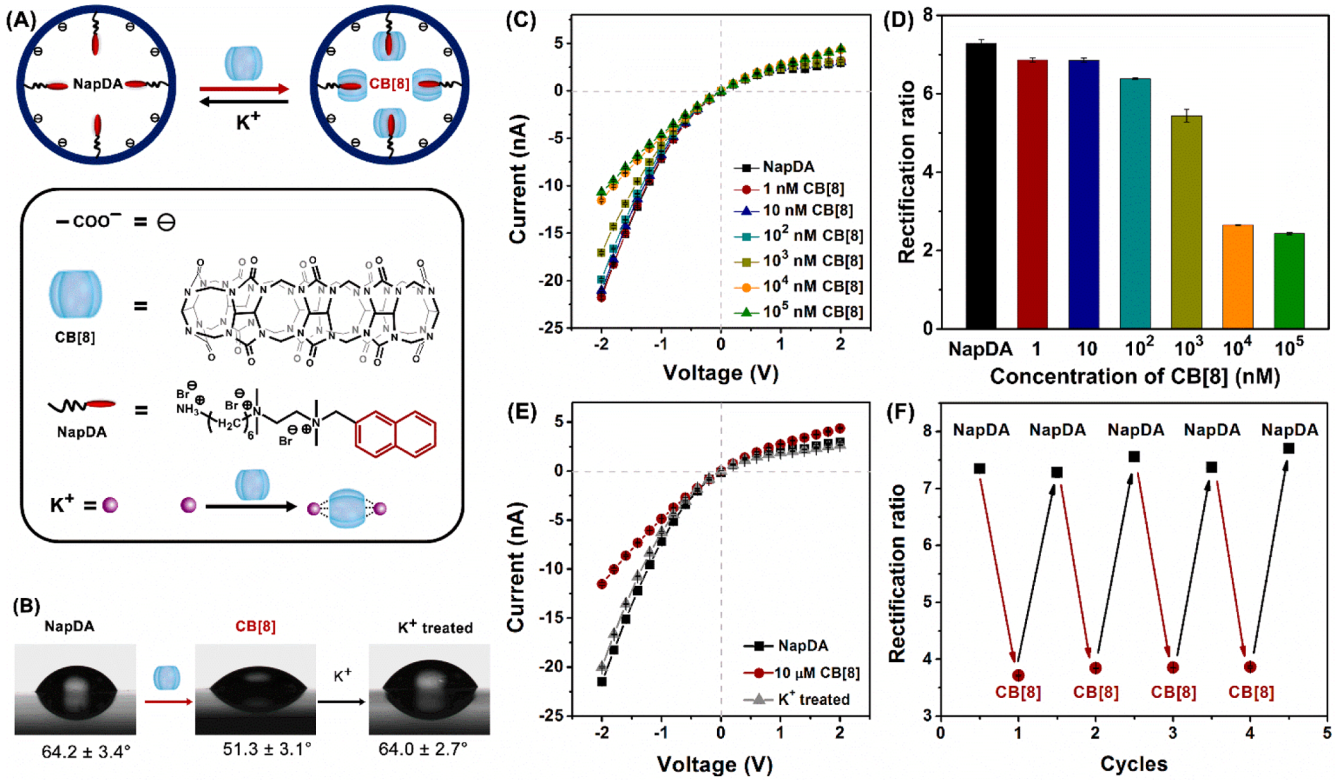

Figure 1. Reversible gating of the NapDA-modified nanochannel between two different rectification states by CB[8] and K^+. (A) Schematic representation of reversible binding of CB[8] inside the NapDA-modified nanochannel. Binding of CB[8] produced the CB[8]-bound state. K^+ can bind with CB[8], as shown in the lower panel, thus removing CB[8] from the nanochannel and getting the primary NapDA-modified state back. (B) Reversible change of the contact angle of NapDA-modified PET membrane by CB[8] and K^+. The $I-V$ curves (C) and rectification ratios (ratio = $|I_{-2\ V}|/I_{+2\ V}$) (D) of NapDA-modified nanochannel gated by different concentrations of CB[8] (from 1 nM to 100 μM of CB[8]). As the concentration of CB[8] increased, the current at −2 V and rectification ratio decreased gradually. (E) $I-V$ curves of the NapDA-modified nanochannel measured in 0.1 M NaCl solutions without and with 10 μM CB[8]. The ion current and rectification ratio of the channel almost completely recovered after removing CB[8] molecules from the channel surface by K^+. (F) Reversible switching of the rectification ratios of the channel between two different rectification states, namely NapDA-modified and CB[8]-bound states.

M^{-2}, such a strong interaction has been used to drive supramolecular self-assemblies at very low concentrations.[42,43] Furthermore, layer-by-layer (LbL) self-assembly has been proved to be a convenient and powerful method to construct multilayer films on surfaces.[44−47] Recently, our group demonstrated that host-enhanced $\pi-\pi$ interaction could be utilized to construct supramolecular networks on substrates by an LbL method, through rational molecular design, and the formed films were endowed with various functions.[48,49]

Herein, reversible and adjustable multiple gating states of a single nanochannel have been realized through a nanoconfined supramolecular self-assembly method. To achieve supramolecular self-assembly inside the nanochannel, the surface of the nanochannel was first modified by a self-assembly precursor. Then, through an LbL method, host and guest molecules were self-assembled onto the nanochannel surface driven by host−guest interaction, forming monolayer or multilayers. Through well controlling the number of the self-assembled layers in the nanochannel, multiple stable gating states were realized. By alternately adding competing guest molecules and building blocks, the LbL gating states can be eliminated and recovered cyclically. This work provides a new approach for enhancing functionalities of artificial nanochannels by LbL supramolecular self-assemblies. Based on the reversible and adjustable multiple gating states, different surface properties and sizes of the nanochannel can be realized, thus various functions can be integrated in a single nanochannel.

RESULTS AND DISCUSSION

A single asymmetrically conical nanochannel embedded within polyethylene terephthalate (PET) membrane was fabricated through an ion track etching method assisted with surfactant.[50] In consideration of the difficulty in locating the channel on a single-channel membrane under a scanning electron microscope (SEM), a multichannel membrane with channel density of 10^8 cm^{-2} was prepared under the same conditions as the single-nanochannel membrane, and it was characterized by SEM to confirm the asymmetric geometry of the channel. SEM images showed that the diameter of the large base side was 186 ± 28 nm, whereas the diameter of the smaller tip side was 31 ± 12 nm (Figure S1 in Supporting Information). This result indicates the asymmetrical structure of the nanochannel. The asymmetric structure and the COOH groups on the channel, generated during chemical etching process, resulted in a rectification effect of the conical nanochannel, characterized as asymmetric current−voltage ($I-V$) curve observed in 0.1 M NaCl solution (Figure S2 in Supporting Information). This diode-like conical nanochannel preferentially transported cations from the tip to the base of the channel.

To realize the gating of the conical nanochannel through supramolecular self-assembly, we designed and synthesized N1-

DOI: 10.1021/jacs.6b09601
J. Am. Chem. Soc. 2016, 138, 16372−16379

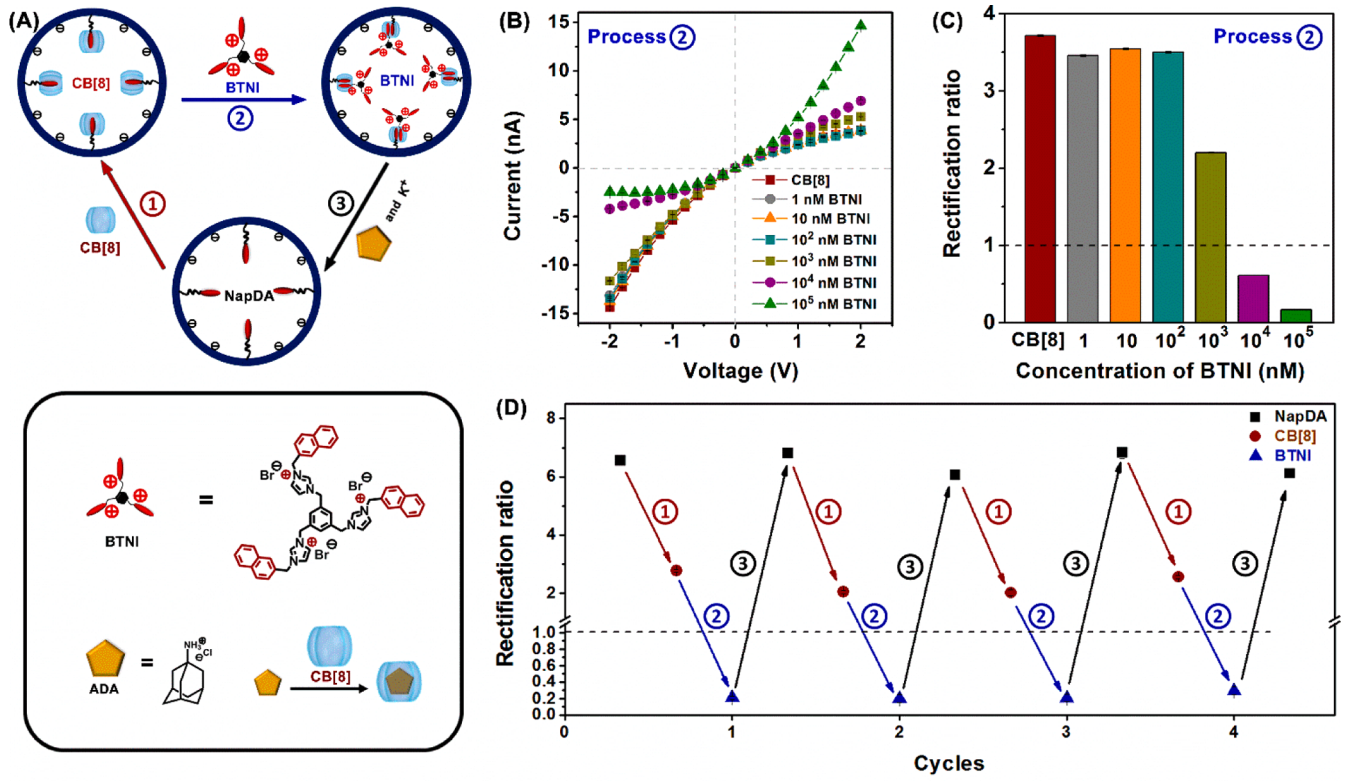

Figure 2. Reversible and adjustable three-state gating of the nanochannel by self-assembly of BTNI and CB[8]. (A) Reversible binding of CB[8] and BTNI inside NapDA-modified nanochannel. Process ①: Binding of CB[8] inside NapDA-modified nanochannel, producing the CB[8]-bound state. Process ②: Binding of BTNI inside CB[8]-bound nanochannel, producing the BTNI-bound state. Process ③: ADA can bind with CB[8] through host−guest interaction, as shown in the lower panel. Thus, ADA and K^+ can jointly remove CB[8] and BTNI from the nanochannel, getting the primary NapDA-modified state back. (B, C) For process ②, the concentration dependence of BTNI-gating inside CB[8]-bound nanochannel. The *I*−*V* curves (B) and rectification ratios (C) of CB[8]-bound nanochannel gated by different concentrations of BTNI (from 1 nM to 100 μM of BTNI). As the concentration of BTNI increased, the current at −2 V and rectification ratio decreased gradually. (D) Reversible cycles of rectification ratio of the nanochannel under the NapDA-modified state, CB[8]-bound state, and BTNI-bound state, through processes ①, ②, and ③.

(2-(dimethyl(naphthalen-2-ylmethyl)ammonio)-ethyl)-N1,N1-dimethylhexane-1,6-diaminium (NapDA) (Figure S3A in Supporting Information) and further used it to modify the inner surface of the nanochannel as a self-assembly precursor to drive the supramolecular self-assembly. NapDA molecule possessed an amino group on one end to react with the COOH group on the channel surface (Figure S4A in Supporting Information) and a naphthalene group on the other end, for further binding with CB[8] by host−guest interaction. The covalent modification was confirmed by contact angle (CA) and X-ray photoelectron spectroscopy (XPS) experiments (see Figure S4B−E and Tables S1 and S2 in Supporting Information). The ion transport property of the nanochannel before and after modification was characterized by transmembrane ion current measurement under 0.1 M NaCl solution (Figure S5 in Supporting Information). After modification, due to the reduction of effective negative charges on the nanochannel surface by the positive charges of NapDA molecules, both ionic current and rectification ratio (ratio = $|I_{-2\ V}|/I_{+2\ V}$) of the channel lowered, which also confirmed that the NapDA was successfully grafted onto the channel surface.

Based on the NapDA molecules immobilized on the channel surface, primary supramolecular gating of the NapDA-modified nanochannel between two different states was achieved by CB[8] and K^+ (Figure 1A). After immersing the nanochannel in an aqueous solution of CB[8], CB[8] was noncovalently bound onto the channel surface by host−guest interaction, which was confirmed by CA measurement (Figure 1B). CB[8] exhibited a gating effect with a concentration dependence, as indicated by the *I*−*V* curve and rectification ratio changes of the channel under different CB[8] concentrations. As shown in Figure 1C,D, as the concentration of CB[8] increased, the *I*−*V* curve and rectification ratio remained the same at the scale of 1−100 nM. From 100 nM to 10 μM, both the current at −2 V and the rectification ratio decreased as the concentration increased. From 10 μM to 100 μM, the current at −2 V and the rectification ratio changed slightly. These results indicate that the ion transport property of the NapDA-modified nanochannel is dependent on the concentration of CB[8]. The concentration of 10 μM was chosen for other CB[8]-related gating experiment. To demonstrate that CB[8] was bound to NapDA rather than physically adsorbed by the original nanochannel surface, the ion transport property of the unmodified nanochannel under different concentrations of CB[8] was investigated. As the concentration of CB[8] increased, *I*−*V* curves and rectification ratios of the unmodified nanochannel did not change (Figure S6 in Supporting Information). This gating effect was caused by the noncovalent modification of CB[8], which should influence the nanochannel by reducing the effective channel diameter and shielding the negative charged COOH groups due to CB[8]'s relatively large size.[51] The mechanism for the dependence of *I*−*V* curve and rectification ratio of the nanochannel on CB[8] concentration was analyzed in detail (see Figure S7 and Table S3 in

DOI: 10.1021/jacs.6b09601
J. Am. Chem. Soc. 2016, 138, 16372−16379

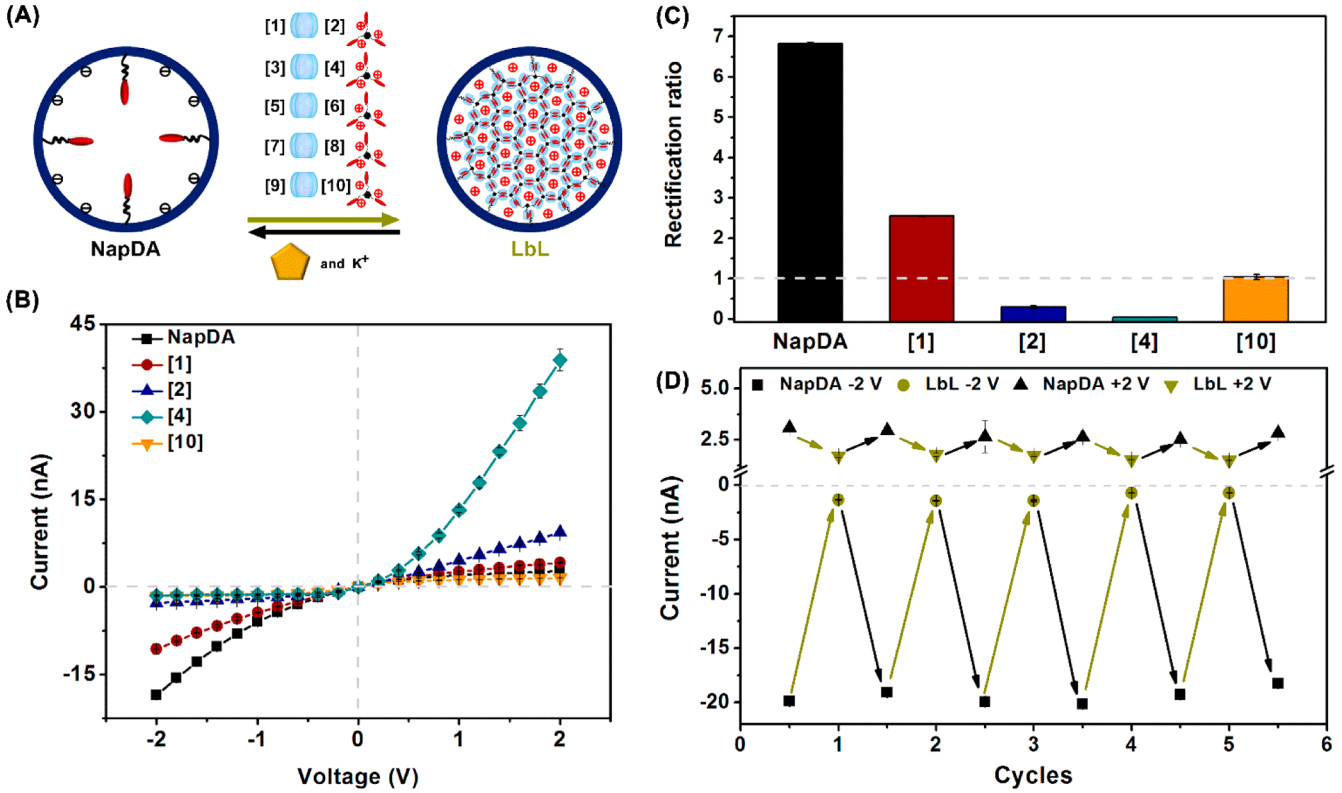

Figure 3. Reversible and adjustable multiple gating states of the NapDA-modified single nanochannel through the LbL self-assembly of CB[8] and BTNI into the channel. (A) CB[8] and BTNI could be self-assembled into a NapDA-modified nanochannel through the LbL self-assembly method, finally forming a supramolecular network inside the nanochannel. As the number of layers grew, different gating states could be realized ([1] state: $CB[8]_1BTNI_0$, [2] state: $CB[8]_1BTNI_1$, [3] state: $CB[8]_2BTNI_1$, [4] state: $CB[8]_2BTNI_2$, [5] state: $CB[8]_3BTNI_2$, [6] state: $CB[8]_3BTNI_3$, [7] state: $CB[8]_4BTNI_3$, [8] state: $CB[8]_4BTNI_4$, [9] state: $CB[8]_5BTNI_4$, [10] state: $CB[8]_5BTNI_5$). For clarity, *I*−*V* curves (B) and rectification ratios (C) of five selected gating states, namely, the primary NapDA-modified state, [1], [2], [4], and [10] states, are shown. The five states exhibited different ion transport properties. As the assembled layers of CB[8] and BTNI grew, the current at −2 V gradually decreased, and the rectification ratio decreased to <1, then increased to around 1. After self-assembly of several layers of CB[8] and BTNI onto the channel surface (such as state [10]), the transmembrane ion current of the nanochannel decreased to a quite low value at both positive and negative voltage, and the rectification ratio changed to around 1, which indicates an effective blocking effect. (D) Reversible cycles of currents at −2 V and +2 V of the nanochannel between the primary NapDA-modified and [10] states.

Supporting Information). Therefore, CB[8] can exhibit a supramolecular gating effect with a concentration dependence, through host−guest interaction driven self-assembly inside the NapDA-modified nanochannel.

The CB[8]-gated nanochannel also exhibited good stability and reversibility. In water, CB[8] can interact with K^+ ions.[52,53] When treating the CB[8]-bound channel with K^+ solution, K^+ ions can bind with CB[8] molecules, thus removing it from the nanochannel (Figure 1A). As shown in Figure 1B, CA measurement of NapDA-modified PET film confirmed the reversible binding of CB[8]. Moreover, the *I*−*V* curve of the channel almost completely recovered after washing the channel with 1 M K^+ solution (Figure 1E). The influence of K^+ concentration on the nanochannel recovery was also well characterized in Figure S8, Supporting Information. The rectification ratio of the channel at 2 V reversibly switched between 7.45 ± 0.17 and 3.82 ± 0.07 for at least four cycles as the formation and removal of CB[8]-gating, and no damping was observed (Figure 1F). Therefore, the CB[8]-gating possesses good reversibility and cycling performance to regulate the ion transport property of the nanofluidic diode.

The monolayer CB[8]-gating provides a chance for achieving reversible multiple gating states through the LbL self-assembly method. Here, primarily, we attempt to build the second layer in the nanochannel for a three-state gating function. As shown in Figure 2A, through three processes, a three-state gating cycle can be realized. After CB[8]-gating (process ①), a three-armed naphthalene derivative can bind with the CB[8] inside the nanochannel (process ②), resulting in the change of the ion transport property, then adamantanamine hydrochloride (ADA) and K^+ can jointly remove CB[8] and BTNI from the nanochannel (process ③), getting the nanochannel back to the NapDA-modified state.[48] ADA can bind with CB[8] with a binding constant much higher than K^+,[48,54] because the supramolecular self-assembly of CB[8] and BTNI inside the nanochannel was much more stable than the CB[8] monolayer film, and ADA was added to accelerate the removement process. Process ① has been discussed as the CB[8]-gating in Figure 1. For process ②, the three-armed naphthalene derivative, 1,1′,1″-(benzene-1,3,5-triyltris(methylene))tris(3-(naphthalen-2-ylmethyl)-1H-imidazol-3-ium)bromide (BTNI), was designed and synthesized (see Figure S3B in Supporting Information). As confirmed by CA measurement (Figure S9 in Supporting Information), BTNI can bind onto a CB[8]-bound PET substrate, indicating that BTNI can also bind onto a CB[8]-bound nanochannel surface, shown schematically as process ② in Figure 2A. The binding of BTNI resulted in a gating effect with a concentration dependence, as shown by the

DOI: 10.1021/jacs.6b09601
J. Am. Chem. Soc. 2016, 138, 16372−16379

change of $I-V$ curve and rectification ratio of the nanochannel under different BTNI concentrations (Figure 2B,C). As the concentration of BTNI increased, the current at −2 V (Figure 2B) and the rectification ratio (Figure 2C) remained the same at the very beginning and then decreased gradually. Different from CB[8]-gating of the channel, the rectification ratio of BTNI gating state became <1 at high BTNI concentrations (Figure 2C), indicating that the rectification direction of the nanochannel was reversed at such concentrations. This is mainly because the positively charged BTNI molecules could reverse the net surface charge of the channel from negative to positive, which favored an opposite ion current rectification. Similar to CB[8]-gating, the concentration dependence of BTNI-gating should be also due to the dynamic nature of host-enhanced $\pi-\pi$ interaction. Therefore, the ion transport property, especially the rectification degree and direction, can be regulated through BTNI-gating (process ②) with a concentration dependence.

The reversible gating process of the diode among NapDA-modified, CB[8]-bound, and BTNI-bound states can be realized by the combination of CB[8], BTNI, K^+, and ADA, shown schematically as processes ①, ②, and ③ in Figure 2A. In process ③, we used 1 M K^+ and 1 mM ADA to wash the channel twice to effectively remove CB[8] and BTNI. The whole reversible process was characterized by the rectification ratio of each state. As shown in Figure 2D, reversible changing of rectification ratio of each state among ∼6.5, ∼2.5, and ∼0.2 for at least four cycles confirmed that the channel could be cyclically and reversibly switched among three ion conduction states.

In this context, reversible, stable, and adjustable multiple gating states of a single nanochannel were further realized through the LbL self-assembly method (Figure 3A). According to the LbL self-assembly method, the NapDA-modified nanochannel was alternately immersed into aqueous solution of 10 μM CB[8] with 0.1 M NaCl and 10 μM BTNI with 0.1 M NaCl, and each assembled layer could produce a new ion conduction state ([1] state: $CB[8]_1BTNI_0$, [2] state: $CB[8]_1BTNI_1$, [3] state: $CB[8]_2BTNI_1$, [4] state: $CB[8]_2BTNI_2$, [5] state: $CB[8]_3BTNI_2$, [6] state: $CB[8]_3BTNI_3$, [7] state: $CB[8]_4BTNI_3$, [8] state: $CB[8]_4BTNI_4$, [9] state: $CB[8]_5BTNI_4$, [10] state: $CB[8]_5BTNI_5$), then ADA and K^+ jointly removed CB[8] and BTNI from the nanochannel, getting the nanochannel back to the NapDA-modified state. The $I-V$ curves and rectification ratios of all the gating states are shown in Figure S10 in Supporting Information. For clarity, the primary NapDA-modified state and the four other states ([1], [2], [4], and [10] states) were chosen for multiple state demonstration. As shown in Figure 3B,C, the $I-V$ curves and rectification ratios of the five states were different from each other, indicating that the five gating states possessed different ion transport properties. As the assembled layers of CB[8] and BTNI grew, the current of the nanochannel at −2 V reduced from ∼−18.53 nA (NapDA-modified state) to ∼−0.98 nA ([10] state), because of the increase of positive charge on the nanochannel surface and the decrease of the effective diameter. The rectification ratio of nanochannel first decreased from ∼6.83 (NapDA-modified state) to ∼0.04 ([4] state), due to the increase of the positive charge on the nanochannel surface, and then increased to around 1 ([10] state), because the self-assembled layers blocked the nanochannel, making it more symmetrical. Therefore, the ion transport property of nanochannel can be regulated among multiple gating states through the LbL method.

The reversibility between the complete blocking state-[10] and NapDA-modified state also can be achieved by K^+ and ADA, as shown in Figure 3A. As shown in Figure 3D, the ion currents of the nanochannel at −2 V and +2 V were cyclically switched between high and low ion-conduction states via the removal and formation of supramolecular multilayers ([10] state) in the nanochannel. After switching for at least 5 cycles, no obvious change of the ion conduction under each gating state was observed. The above results demonstrate that the supramolecular gating of the nanochannel by the LbL self-assembly method has good reversibility and cycling performance.

To characterize the stability of the multiple gating states, $I-t$ curves of NapDA-modified state, [1], [2], [4], and [10] states were measured at different voltages. As shown in Figure 4, at

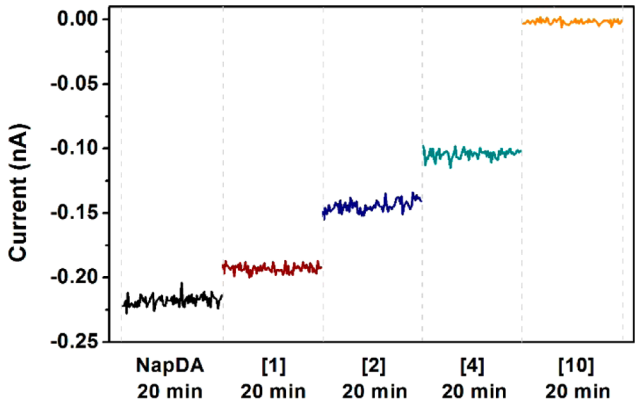

Figure 4. Currents at −0.2 V for each gating state stayed the same for at least 20 min, indicating the high stability of the gating states.

−0.2 V, each state could remain stable for 20 min, which is long enough for testing in a practical application. In fact, all the states can remain stable for at least 1 h (Figure S11, Supporting Information). The current decreased as the layers grew, this was mainly because the growing layers reduced the effective diameter of the nanochannel, this trend was the same in the range from −0.4 V to −1 V. Therefore, the multiple gating states of single nanochannel are stable, and the current of each state changes monotonously with the number of self-assembly layers in a wide voltage range.

Different from the multiple gating states here, in most previously reported works about functional nanochannels, the nanochannel can be only modified by one layer of functional molecules or polymers,[2,3,7,12,22] and the surface charge density and polarity, the effective size, and the geometric asymmetry are fixed once the nanochannels are modified, thus their gating states cannot be further regulated. CB[8] can encapsulate different kinds of species,[54,55] including a great number of stimuli-responsive molecules, thus when the multiple gating states are combined with these molecules, stimuli responsiveness with different sensitivity and range of response should be realized, corresponding to different original gating states. Therefore, this work can be developed for novel stable multiple-state functional nanofluidic devices.

We wondered if the LbL self-assembly had an advantage in realizing a blocking effect over direct adsorption of preformed hyperbranched supramolecular networks into the nanochannel. To answer this question, the nanochannel was immersed in a

DOI: 10.1021/jacs.6b09601
J. Am. Chem. Soc. 2016, 138, 16372−16379

mixed solution of CB[8] and BTNI, which contained many groups of preformed hyperbranched supramolecular networks driven by host-enhanced $\pi-\pi$ interaction (Figure 5A).[56] A

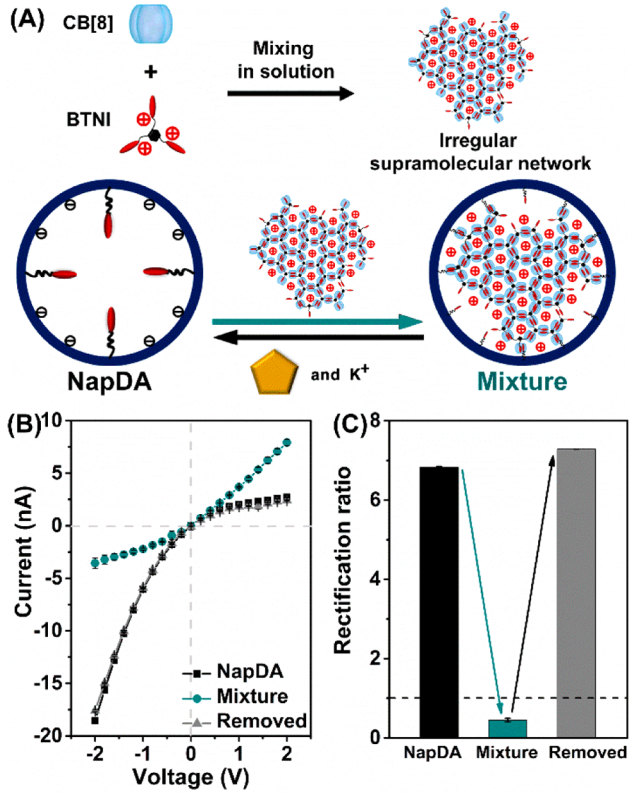

Figure 5. Reversible gating of single nanochannel by a preformed network of CB[8] and BTNI. (A) CB[8] (10 μM) and BTNI (10 μM) were mixed in water to form a CB[8]-BTNI network through host-enhanced $\pi-\pi$ interaction. NapDA-modified nanochannel was immersed in this mixture solution, and the supramolecular networks could be immobilized into the channel and realized gating effect. $I-V$ curves (B) and rectification ratios (C) of the NapDA-modified nanochannel without and with the binding of supramolecular networks. After addition of the positively charged network, the current at −2 V decreased, and the rectification direction reversed. After removal of the network, the $I-V$ curve and rectification ratio almost completely recovered.

solution of 10 μM CB[8], 10 μM BTNI, and 0.1 M NaCl was prepared, and the concentrations were determined to keep up with previous conditions for the CB[8]-gating and BTNI-gating. As shown in Figure S12, Supporting Information, through measuring by dynamic light scattering (DLS) in solution, the average diameter of the networks was about 62 nm, which was smaller than the base but larger than the tip diameter of the single nanochannel. As a result, the networks could enter the nanochannel from the base side and bind with the channel wall, and thus change ion transport property. After the NapDA-modified nanochannel was immersed in this solution, the $I-V$ curve was measured to characterize the change of ion transportation property. As shown in Figure 5B,C, the current at −2 V decreased, and the rectification ratio became <1. This gating effect mainly resulted from the positive charge of the network, which reversed the charge polarity of the nanochannel surface. K^+ and ADA can also destroy the mixture-gating through binding with CB[8], which endows mixture-gating with good reversibility (Figure 5B,C). But it can hardly realize reversible cycles, because for each cycle, the entered networks should be different in shape and size. The current of mixture-gating is much higher than that of the [10] state at both −2 V and +2 V, indicating that the blocking effect of this mixture-gating is much weaker than LbL-gating. This is mainly because in the mixture-gating method, the preformed irregular networks cannot match up well with the single nanochannel in shape (Figure 5A), thus the network cannot fully fill the nanochannel.

The on−off ratio reflects the blocking effect of each gating, which is calculated through dividing the current of the NapDA-modified nanochannel by the current of each gating state at −2 V and +2 V, respectively. As shown in Figure 6A,B, at −2 V, the

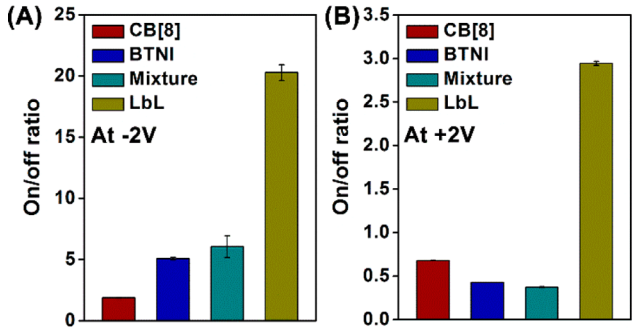

Figure 6. On−off ratios of CB[8]-gating, BTNI-gating, mixture-gating, and LbL-blocking state ([10] state) at (A) −2 V and (B) + 2 V. The on−off ratio is calculated through dividing the current of the NapDA-modified nanochannel by the current of each gating state. The results demonstrate that the best blocking effect is realized at the LbL-blocking state.

on−off ratios of the gatings by CB[8], BTNI, mixture, and LbL method ([10] state) are about 1.9, 5.1, 6.0, and 20.3, respectively. At + 2 V, the on−off ratios of the gatings by CB[8], BTNI, mixture, and LbL method are about 0.7, 0.4, 0.4, and 2.94, respectively. At both −2 V and +2 V, the on−off ratios of LbL-blocking state ([10] state) are much higher than that of other gating states, indicating that LbL self-assembly is the most effective method to achieve a blocking effect.

CONCLUSIONS

In summary, reversible and adjustable multiple gating states of a single nanochannel have been realized through the nano-confined supramolecular self-assembly method. The supramolecular self-assembly was driven by host-enhanced $\pi-\pi$ interaction, and the procedure was simply an immersion of the single nanochannel in aqueous solutions of self-assembly building blocks for only 10 min at room temperature. Through LbL method, the ion transport property of nanochannel was regulated among stable multiple states, and blocking effect was realized after several layers of LbL self-assembly. The gating effects are mainly determined by charge and steric effects. These gating effects are highly reversible, and each gating can be reproduced for many cycles. This study provides a new method for simultaneously regulating steric structure and charge distribution in nanochannels and thus realizing reversible and adjustable multiple gating states. Furthermore, this work can be extended to build a diverse stable multiple-state research platform for various supramolecular systems, employing other host−guest interactions, for example, cyclo-

DOI: 10.1021/jacs.6b09601
J. Am. Chem. Soc. 2016, 138, 16372−16379

dextrin, crown ether, and calixarene-based host−guest interactions.

EXPERIMENTAL SECTION

Materials. Benzyl(6-bromohexyl)carbamate (97%) and 1,3,5-tris((1H-imidazol-1-yl)methyl)benzene were purchased from TCI. HAc/HBr (HBr wt % = 33%), ADA, N^1,N^1,N^2,N^2-tetramethylethane-1,2-diamine (98%) and 2-(bromomethyl)naphthalene (95%) were purchased from J&K Scientific. 1-(3-(Dimethylamino)propyl)-3-ethylcarbodiimide hydrochloride (EDC) (95%) and *N*-hydroxysulfosuccinimide sodium salt (NHSS) (95%) were purchased form Alfa Aesar. CB[8] was purchased from Sigma-Aldrich.

NMR Spectra. ^{1}H NMR and ^{13}C NMR spectra was recorded on a JEOL JNM-ECA400 apparatus (400 MHz).

CA Measurement. Contact angles were measured using an OCA20 (DataPhysics, Germany) contact-angle system at room temperature. Before measurement, the sample was dried by N_2 flow. In each measurement, 2 μL water was dispensed onto the sample substrate. The contact angle was the average value of 10 different drops.

XPS Measurement. XPS data were measured by an ESCALab220i-XL electron spectrometer from VG Scientific using 300W Al Kα radiation, and the base pressure was about 3×10^{-9} mbar. The binding energy was defined taking C 1s peak at 284.8 eV as a reference.

Nanochannel Preparation. PET membranes (Hostaphan RN12 Hoechst, 12 μm thick, with single or multiple ion tracks in the center) were etched from one side with 6 M NaOH and from the other side with etching solution (6 M NaOH + 0.025% sodium dodecyl diphenyloxide disulfonate) at 60 °C to produce single or multiple cone-shaped nanochannels. To observe the etching process, a picoammeter was employed. The etching process was stopped by addition of a mixture of 1 M KCl and 1 M HCOOH aqueous solution that was able to neutralize the base solution. The profiles and diameters of the nanochannels were observed by SEM from the multichannel membranes produced in the same etching process as single channel membranes.

Modification of NapDA in Nanochannel. An aqueous solution of 3 mg/mL NHSS and 15 mg/mL EDC was prepared as an activator. The single nanochannel membrane was immersed into it. One hour later, the membrane was moved to 1 mM NapDA aqueous solution for amidation reaction. After 8 h, the membrane was taken out and then immersed in water for 5 min to remove residue reagents.

Current Measurement. The current measurements were carried out with a Keithley 6487 picoammeter (Keithley Instruments, Cleverland, OH), and the PET membrane with a single nanochannel was located between two cells. Two Ag/AgCl electrodes were placed in both cells, respectively, and employed to apply a voltage across the membrane. The anode faced the base side of the nanochannel. A scanning voltage from −2 V to +2 V with a period of 20 s was determined. For the measurements of different nanochannels, a different solution with 0.1 M NaCl was chosen. For example, a solution of 10 μM CB[8] and 0.1 M NaCl was added to both sides of the membrane to evaluate the ion transport property change by CB[8]-gating.

ASSOCIATED CONTENT

Supporting Information

The Supporting Information is available free of charge on the ACS Publications website at DOI: 10.1021/jacs.6b09601.

Details of fabrication and SEM image, CA change, XPS data, ion current measurement of the nanochannel before and after modification by NapDA, synthetic routes and characterization of the chemicals, CA changes, and XPS data for CB[8]-gating and BTNI-gating, mechanism of concentration dependence of the gatings, *I*−*V* curve change and rectification ratio change during the LbL self-assembly process, time-dependent current of NapDA-modified state, [1], [2], [4], and [10] states at −0.2 V (PDF)

AUTHOR INFORMATION

Corresponding Authors

*tianyely@iccas.ac.cn
*xi@mail.tsinghua.edu.cn
*jianglei@iccas.ac.cn

ORCID

Huanting Wang: 0000-0002-9887-5555
Lei Jiang: 0000-0003-4579-728X

Author Contributions

‡These authors contributed equally.

Notes

The authors declare no competing financial interest.

ACKNOWLEDGMENTS

National Natural Science Foundation (21421064, 21501185, 21421061) and National Basic Research Program of China (2013CB834502, 2013CB932802).

REFERENCES

(1) Sparreboom, W.; van den Berg, A.; Eijkel, J. C. T. *Nat. Nanotechnol.* **2009**, *4*, 713.
(2) Hou, X.; Guo, W.; Jiang, L. *Chem. Soc. Rev.* **2011**, *40*, 2385.
(3) Zhang, H. C.; Tian, Y.; Jiang, L. *Nano Today* **2016**, *11*, 61.
(4) Dekker, C. *Nat. Nanotechnol.* **2007**, *2*, 209.
(5) Siwy, Z.; Heins, E.; Harrell, C. C.; Kohli, P.; Martin, C. R. *J. Am. Chem. Soc.* **2004**, *126*, 10850.
(6) White, R. J.; Ervin, E. N.; Yang, T. L.; Chen, X.; Daniel, S.; Cremer, P. S.; White, H. S. *J. Am. Chem. Soc.* **2007**, *129*, 11766.
(7) Xia, F.; Guo, W.; Mao, Y. D.; Hou, X.; Xue, J. M.; Xia, H. W.; Wang, L.; Song, Y. L.; Ji, H.; Ouyang, Q.; Wang, Y. G.; Jiang, L. *J. Am. Chem. Soc.* **2008**, *130*, 8345.
(8) Yameen, B.; Ali, M.; Neumann, R.; Ensinger, W.; Knoll, W.; Azzaroni, O. *J. Am. Chem. Soc.* **2009**, *131*, 2070.
(9) Madrid, E.; Rong, Y. Y.; Carta, M.; McKeown, N. B.; Malpass-Evans, R.; Attard, G. A.; Clarke, T. J.; Taylor, S. H.; Long, Y. T.; Marken, F. *Angew. Chem., Int. Ed.* **2014**, *53*, 10751.
(10) Wang, G. L.; Zhang, B.; Wayment, J. R.; Harris, J. M.; White, H. S. *J. Am. Chem. Soc.* **2006**, *128*, 7679.
(11) Hou, X.; Guo, W.; Xia, F.; Nie, F. Q.; Dong, H.; Tian, Y.; Wen, L. P.; Wang, L.; Cao, L. X.; Yang, Y.; Xue, J. M.; Song, Y. L.; Wang, Y. G.; Liu, D. S.; Jiang, L. *J. Am. Chem. Soc.* **2009**, *131*, 7800.
(12) Xie, G. H.; Xiao, K.; Zhang, Z.; Kong, X. Y.; Liu, Q.; Li, P.; Wen, L. P.; Jiang, L. *Angew. Chem., Int. Ed.* **2015**, *54*, 13664.
(13) Siwy, Z.; Powell, M. R.; Petrov, A.; Kalman, E.; Trautmann, C.; Eisenberg, R. S. *Nano Lett.* **2006**, *6*, 1729.
(14) Harrell, C. C.; Kohli, P.; Siwy, Z.; Martin, C. R. *J. Am. Chem. Soc.* **2004**, *126*, 15646.
(15) Gao, P.; Martin, C. R. *ACS Nano* **2014**, *8*, 8266.
(16) Buchsbaum, S. F.; Nguyen, G.; Howorka, S.; Siwy, Z. *J. Am. Chem. Soc.* **2014**, *136*, 9902.
(17) Seifert, A.; Göpfrich, K.; Burns, J. R.; Fertig, N.; Keyser, U. F.; Howorka, S. *ACS Nano* **2015**, *9*, 1117.
(18) Liu, Q.; Wen, L. P.; Xiao, K.; Lu, H.; Zhang, Z.; Xie, G. H.; Kong, X.-Y.; Bo, Z. S.; Jiang, L. *Adv. Mater.* **2016**, *28*, 3181.
(19) Zhou, Y. H.; Guo, W.; Cheng, J. S.; Liu, Y.; Li, J. H.; Jiang, L. *Adv. Mater.* **2012**, *24*, 962.
(20) Zhang, J. T.; Liu, N. N.; Wei, B. M.; Ou, X. W.; Xu, X. M.; Lou, X. D.; Xia, F. *Chem. Commun.* **2015**, *51*, 10146.
(21) Zhang, M. H.; Hou, X.; Wang, J. T.; Tian, Y.; Xia, F.; Zhai, J.; Jiang, L. *Adv. Mater.* **2012**, *24*, 2424.
(22) Vlassiouk, I.; Park, C. D.; Vail, S. A.; Gust, D.; Smirnov, S. *Nano Lett.* **2006**, *6*, 1013.

DOI: 10.1021/jacs.6b09601
J. Am. Chem. Soc. 2016, 138, 16372−16379

(23) Xie, G. H.; Tian, W.; Wen, L. P.; Xiao, K.; Zhang, Z.; Liu, Q.; Hou, G. L.; Li, P.; Tian, Y.; Jiang, L. *Chem. Commun.* **2015**, *51*, 3135.
(24) Han, C. P.; Hou, X.; Zhang, H. C.; Guo, W.; Li, H. B.; Jiang, L. *J. Am. Chem. Soc.* **2011**, *133*, 7644.
(25) Ali, M.; Ahmed, I.; Ramirez, P.; Nasir, S.; Niemeyer, C. M.; Mafe, S.; Ensinger, W. *Small* **2016**, *12*, 2014.
(26) An, N.; Fleming, A. M.; White, H. S.; Burrows, C. J. *ACS Nano* **2015**, *9*, 4296.
(27) Guo, W.; Hong, F.; Liu, N. N.; Huang, J. Y.; Wang, B. Y.; Duan, R. X.; Lou, X. D.; Xia, F. *Adv. Mater.* **2015**, *27*, 2090.
(28) Li, S. J.; Li, J.; Wang, K.; Wang, C.; Xu, J. J.; Chen, H. Y.; Xia, X. H.; Huo, Q. *ACS Nano* **2010**, *4*, 6417.
(29) Pérez-Mitta, G.; Marmisollé, W. A.; Trautmann, C.; Toimil-Molares, M. E.; Azzaroni, O. *J. Am. Chem. Soc.* **2015**, *137*, 15382.
(30) Zhang, H. C.; Tian, Y.; Hou, J.; Hou, X.; Hou, G. L.; Ou, R. W.; Wang, H. T.; Jiang, L. *ACS Nano* **2015**, *9*, 12264.
(31) Wang, H. Y.; Ying, Y. L.; Li, Y.; Kraatz, H. B.; Long, Y. T. *Anal. Chem.* **2011**, *83*, 1746.
(32) Powell, M. R.; Sullivan, M.; Vlassiouk, I.; Constantin, D.; Sudre, O.; Martens, C. C.; Eisenberg, R. S.; Siwy, Z. *Nat. Nanotechnol.* **2008**, *3*, 51.
(33) Chen, W.; Wu, Z. Q.; Xia, X. H.; Xu, J. J.; Chen, H. Y. *Angew. Chem., Int. Ed.* **2010**, *49*, 7943.
(34) Balzani, V.; Credi, A.; Venturi, M. *ChemPhysChem* **2008**, *9*, 202.
(35) Muratsugu, S.; Tada, M. *Acc. Chem. Res.* **2013**, *46*, 300.
(36) Ahn, Y. J.; Jang, Y. J.; Selvapalam, N.; Yun, G.; Kim, K. *Angew. Chem., Int. Ed.* **2013**, *52*, 3140.
(37) Banerjee, S.; König, B. *J. Am. Chem. Soc.* **2013**, *135*, 2967.
(38) Chandaluri, C. G.; Pelossof, G.; Tel-Vered, R.; Shenhar, R.; Willner, I. *ACS Appl. Mater. Interfaces* **2016**, *8*, 1440.
(39) Kahn, J. S.; Trifonov, A.; Cecconello, A.; Guo, W. W.; Fan, C. H.; Willner, I. *Nano Lett.* **2015**, *15*, 7773.
(40) Pérez-Mitta, G.; Albesa, A. G.; Knoll, W.; Trautmann, C.; Toimil-Molares, M. E.; Azzaroni, O. *Nanoscale* **2015**, *7*, 15594.
(41) Pérez-Mitta, G.; Burr, L.; Tuninetti, J. S.; Trautmann, C.; Toimil-Molares, M. E.; Azzaroni, O. *Nanoscale* **2016**, *8*, 1470.
(42) Liu, Y. L.; Liu, K.; Wang, Z. Q.; Zhang, X. *Chem. - Eur. J.* **2011**, *17*, 9930.
(43) Liu, Y. L.; Fang, R. C.; Tan, X. X.; Wang, Z. Q.; Zhang, X. *Chem. - Eur. J.* **2012**, *18*, 15650.
(44) Decher, G.; Schlenoff, J. B. *Multilayer Thin Films: Sequential Assembly of Nanocomposite Materials*; Wiley-VCH: Weinheim, Germany, 2003.
(45) Such, G. K.; Johnston, A. P. R.; Caruso, F. *Chem. Soc. Rev.* **2011**, *40*, 19.
(46) Ali, M.; Yameen, B.; Cervera, J.; Ramírez, P.; Neumann, R.; Ensinger, W.; Knoll, W.; Azzaroni, O. *J. Am. Chem. Soc.* **2010**, *132*, 8338.
(47) Ali, M.; Yameen, B.; Neumann, R.; Ensinger, W.; Knoll, W.; Azzaroni, O. *J. Am. Chem. Soc.* **2008**, *130*, 16351.
(48) Yang, H.; Ma, Z.; Yuan, B.; Wang, Z. Q.; Zhang, X. *Chem. Commun.* **2014**, *50*, 11173.
(49) Yuan, B.; Yang, H.; Wang, Z. Q.; Zhang, X. *Langmuir* **2014**, *30*, 15462.
(50) Zhang, H. C.; Hou, X.; Zeng, L.; Yang, F.; Li, L.; Yan, D. D.; Tian, Y.; Jiang, L. *J. Am. Chem. Soc.* **2013**, *135*, 16102.
(51) Kim, J.; Jung, I. S.; Kim, S. Y.; Lee, E.; Kang, J. K.; Sakamoto, S.; Yamaguchi, K.; Kim, K. *J. Am. Chem. Soc.* **2000**, *122*, 540.
(52) Zhang, X. X.; Krakowiak, K. E.; Xue, G. P.; Bradshaw, J. S.; Izatt, R. M. *Ind. Eng. Chem. Res.* **2000**, *39*, 3516.
(53) Liu, Y. L.; Yu, Y.; Gao, J.; Wang, Z. Q.; Zhang, X. *Angew. Chem., Int. Ed.* **2010**, *49*, 6576.
(54) Liu, S. M.; Ruspic, C.; Mukhopadhyay, P.; Chakrabarti, S.; Zavalij, P. Y.; Isaacs, L. *J. Am. Chem. Soc.* **2005**, *127*, 15959.
(55) Barrow, S. J.; Kasera, S.; Rowland, M. J.; del Barrio, J.; Scherman, O. A. *Chem. Rev.* **2015**, *115*, 12320.
(56) Fang, R. C.; Liu, Y. L.; Wang, Z. Q.; Zhang, X. *Polym. Chem.* **2013**, *4*, 900.

DOI: 10.1021/jacs.6b09601
J. Am. Chem. Soc. 2016, 138, 16372−16379